

Evolution of the transverse photoelectron momentum distribution for atomic ionization driven by a laser pulse with varying ellipticity

I. A. Ivanov*

*Research School of Physical Sciences, The Australian
National University, Canberra ACT 0200, Australia*

(Dated: June 21, 2018)

We consider the process of atomic ionization driven by a laser pulse with varying ellipticity. We study distribution of the momenta of the photoelectrons, ionized by a strong laser field, emitted in the direction perpendicular to the polarization plane (transverse distribution). We show, that with changing laser pulse ellipticity, the transverse distribution evolves from the singular cusp-like distribution for the close to linear polarization to the smooth gaussian-like structure for the close to circular polarization. In the latter case, when the ellipticity parameter $\epsilon \rightarrow 1$ the strong-field approximation formula for the transverse momentum distribution becomes quantitatively correct.

I. INTRODUCTION

Tunneling theories of photo-ionization proved to be in the past (and still are) of great importance in understanding atomic or molecular ionization by strong infrared (IR) laser field. By tunneling theories we mean here a broad class of theories comprising original work on the strong-field approximation (SFA) by Keldysh [1], its modification known as Keldysh-Faisal-Reiss (KFR) theory [2, 3], subsequent developments [4–9], or quasistatic theories exploiting the fact, that IR field varies slowly in time [10, 11].

The SFA in its original form [1] did not include any interaction of ejected electron and parental ion. The importance of the effect of the Coulomb field of the parental ion on the ionization process has, however, long been realized. Coulomb field of the residual ion was

*Electronic address: Igor.Ivanov@anu.edu.au

found responsible for such effects as low energy structures in electron spectra [12] or two dimensional momentum distributions [13], Coulomb focusing [14], asymmetry in the spectra of above threshold ionization spectra [15], formation of a cusp in the transverse electron momentum distribution [16].

It is the latter effect, the influence of the Coulomb field of the parental ion on the transverse (i.e. perpendicular to the polarization plane of the driving pulse) electron momentum distribution, which will interest us below. Study of the electron momentum distributions (both in longitudinal and transverse directions) can shed light on fine details of the strong-field ionization process [9, 17].

It has been found [16], that for the case of the linearly polarized laser pulse, the transverse electron momentum distribution exhibits a sharp cusp-like peak at zero transverse momentum. For the case of the circularly polarized light, on the contrary, this distribution was found not to deviate considerably from the gaussian-like structure predicted by the SFA [18]. We see, thus, two different forms (cusp-like and gaussian-like) of the transverse electron momentum distribution for two limiting polarization states of the driving pulse. The aim of the present work is to study transition between these two forms in detail. We shall consider below atom in the field of an elliptically polarized laser pulse, and consider evolution of the transverse electron momentum distribution with varying ellipticity. We use hydrogen atom as a model, atomic units are used throughout the paper.

II. THEORY

We solve the time-dependent Schrödinger equation (TDSE) for a hydrogen atom:

$$i\frac{\partial\Psi(\mathbf{r})}{\partial t} = \left(\hat{H}_{\text{atom}} + \hat{H}_{\text{int}}(t)\right)\Psi(\mathbf{r}). \quad (1)$$

Operator $\hat{H}_{\text{int}}(t)$ in Eq. (1) describes interaction of the atom with the EM field. We use velocity form for this operator:

$$\hat{H}_{\text{int}}(t) = \mathbf{A}(t) \cdot \hat{\mathbf{p}}, \quad (2)$$

with

$$\mathbf{A}(t) = -\int_0^t \mathbf{E}(\tau) d\tau. \quad (3)$$

The laser pulse is elliptically polarized (with ellipticity parameter ϵ), and propagates along the z -direction (assumed to be the quantization axis). Its field components are:

$$E_x = \frac{E}{\sqrt{1+\epsilon^2}} f(t) \cos \omega t \quad , \quad E_y = \frac{E\epsilon}{\sqrt{1+\epsilon^2}} f(t) \sin \omega t \quad . \quad (4)$$

In the calculations presented below we use $E = 0.0534$ a.u., which corresponds to the intensity of 10^{14} W/cm² for the laser pulse described by Eq. (4). For the base frequency of the pulse we use $\omega = 0.057$ a.u. (corresponding to the wavelength of 790 nm). In Eq. (4) the function $f(t) = \sin^2(\pi t/T_1)$ (here T_1 is a total pulse duration) is a pulse envelope. We report below results for the pulse durations $T_1 = 4T$, and $T_1 = 10T$, where $T = 2\pi/\omega$ is an optical cycle of the field (4).

Initial state of the system is the hydrogen ground state. To solve the TDSE we employ the strategy used in the works [19, 20].

Solution of the TDSE is represented as a partial waves series:

$$\Psi(\mathbf{r}, t) = \sum_{l=0}^{L_{\max}} \sum_{\mu=-l}^l f_{l\mu}(r, t) Y_{l\mu}(\theta, \phi). \quad (5)$$

The radial part of the TDSE is discretized on the grid with the stepsize $\delta r = 0.1$ a.u. in a box of the size $R_{\max} = 400$ a.u. for the total pulse duration of 4 optical cycles, and $R_{\max} = 1000$ a.u. for the pulse duration of 10 optical cycles. In the calculations we used $L_{\max} = 50$ in Eq. (5). A series of routine checks ensuring that calculation is well converged with respect to variations of the parameters δr , R_{\max} , and L_{\max} has been performed.

Substitution of the expansion (5) into the TDSE gives us a system of coupled equations for the radial functions $f_{l\mu}(r, t)$, describing evolution of the system in time. To solve this system we use the matrix iteration method developed in [21]. Ionization amplitudes $a(\mathbf{p})$ are obtained by projecting solution of the TDSE at the end of the laser pulse on the set of the ingoing scattering states $\psi_{\mathbf{p}}^{(-)}(\mathbf{r})$ of hydrogen atom.

In the present paper we are interested in the transverse electron momentum distribution, describing probability to detect a photoelectron with a given value of the momentum component p_{\perp} perpendicular to the polarization plane. For the geometry we use $p_{\perp} = p_z$. Transverse momentum distribution can be obtained, therefore, as:

$$W(p_{\perp}) = \int |a(\mathbf{p})|^2 dp_x dp_y \quad (6)$$

The well-known SFA result for the transverse momentum distribution in the case of the elliptically polarized laser pulse is a smooth gaussian form [5]:

$$W(p_{\perp}) \propto \exp \left\{ -\frac{(2I)^{1/2} \sqrt{1 + \epsilon^2}}{E} p_{\perp}^2 \right\}, \quad (7)$$

where I is the ionization potential, and we employ the notation used in Eq. (4) for the laser field parameters.

This smooth distribution is in striking contrast to the cusp-like structure observed in the experiment [16] for the ionization of noble gases by linearly polarized laser field (which corresponds to the case of $\epsilon = 0$ in Eq. (7)). This cusp-like structure has been attributed to the Coulomb effects, which are, of course, neglected in the SFA.

In the next section we shall present results of a systematic study of the perpendicular momentum distributions for various values of the ellipticity parameter ϵ . We shall see, that when ellipticity parameter varies between $\epsilon = 0$ (linear polarization) and $\epsilon = 1$ (circular polarization), spectra evolve from the cusp-like spectra observed in [16] to the gaussian form predicted by the SFA and observed in [18].

III. RESULTS

Figure 1 shows evolution of the distribution $W(p_{\perp})$ with varying ellipticity parameter ϵ , when ionization is driven by a short laser pulse with the duration $T_1 = 4T$ (four optical cycles). A feature of the spectra clearly seen from the Figure 1 is the rapid decline of the transverse distribution with the ellipticity parameter ϵ . This decline agrees with the Eq. (7), which predicts exponential dependence of transverse distribution on the ellipticity parameter for a given field strength, which has the same value $E = 0.0534$ a.u. for all values of ϵ . Another feature clearly seen in the Figure 1 is the gradual transition from the cusp-like structure in the spectra to the smooth gaussian form. As one can see, the cusp-like structure survives till $\epsilon \approx 0.5$.

To gain better insight into this interesting phenomenon we show in Figure 2, Figure 3 the function $V(p_{\perp}) = \log W(p_{\perp})$ for a narrow interval in the vicinity of the singular point $p_{\perp} = 0$. For the distribution $W(p_{\perp})$ to have a cusp at $p_{\perp} = 0$, $V(p_{\perp})$ must clearly be singular there. The nature of this singularity can be guessed from the character of the singularity of $W(p_{\perp})$ seen in Figure 1 for small values of the ellipticity parameter ϵ . One can see, that

$W(p_{\perp})$ is continuous at $p_{\perp} = 0$, but may have infinite derivatives there. Clearly, $V(p_{\perp})$ must possess the same properties. It is natural, therefore, to suggest, that in the vicinity of the singular point $p_{\perp} = 0$ function $V(p_{\perp})$ can be represented as:

$$V(p_{\perp}) = B + A|p_{\perp}|^{\alpha} . \quad (8)$$

We may look at this equation as a tentative expression for the first two terms of an expansion of $V(p_{\perp})$ in the vicinity of the singular point. We perform next a series of the least square fits, fitting the function $V(p_{\perp})$ using Eq. (8), and considering the coefficients A , B , α in this equation as fitting parameters.

Results are shown in Figure 2 and Figure 3. One can see, that Eq. (8) approximates the function $V(p_{\perp})$ in the vicinity of the singular point fairly accurately. The quality of the fit does not depend appreciably on the interval of data we use as an input for the fitting procedure, as long as this interval is sufficiently narrow (results shown in Figure 2 and Figure 3 have been obtained using the interval $p_{\perp} \in (-0.2, 0.2)$ for the fitting procedure). The accuracy of the fit shown in Figure 2, Figure 3 makes the conjecture that Eq. (8) indeed describes faithfully the behavior of $V(p_{\perp})$ in the vicinity of the singular point plausible enough. Further support in favor of the validity of this conjecture is found at a closer inspection of the coefficients of the fitting formula (8), which the fitting procedure gave us.

Fitting parameters A and α describing the character of the singular point are of most interest to us. Their dependence on the ellipticity parameter ϵ is shown in Figure 4. For the nearly circular polarization parameter $\alpha \approx 2$, as prescribed by the tunneling Eq. (7). Moreover, parameter A , as predicted by the tunneling equation, should approach the value $A = -26.48$ for $\epsilon = 1$. We see thus, that for the nearly circular polarization tunneling Eq. (7) describes the electron spectrum fairly accurately. With decreasing values of the ellipticity parameter deviation from the gaussian-like behavior due to the Coulomb effects becomes more and more significant.

This behavior can be understood if we take into account, that the angular momentum composition of the wave function changes considerably with the ellipticity parameter. If we rewrite Eq. (5) as a sum of $\Psi_l(\mathbf{r}, t)$, where each $\Psi_l(\mathbf{r}, t)$ includes only spherical harmonics of rank l , than distribution of the squared norms $N_l = |\Psi_l|^2$ can be used to characterize the angular momentum composition of the wavefunction. Since absorption of a photon from the circularly polarized wave increases magnetic quantum number by one unit, we can expect,

that this distribution will be shifted towards larger l for pulse polarization approaching a circular one. That reasoning is illustrated in Figure 5, where distributions of the norms N_l for the wavefunction after the end of the laser pulse are shown for the cases of $\epsilon = 0$, and $\epsilon = 0.8$. We subtracted contribution of the ground state to the $l = 0$ component. The expected shift towards larger l - values is clearly seen in the Figure 5. This shift towards larger angular momenta means much higher centrifugal barrier, and consequently larger electron-parental ion separation for the close to circular polarization, which should diminish the role of the Coulomb effects.

The role of the high angular momenta can be further clarified, if we consider transverse distributions obtained by putting in Eq. (5) all components of the wavefunction with angular momenta less than certain value L_{\min} , to zero. This means, that projecting the solution of the TDSE on the ingoing scattering states of the hydrogen atom, we ignore all Coulomb continuum wavefunctions with $l < L_{\min}$.

Figure 6 shows the transverse distributions computed for different values of the parameter L_{\min} for the case of the linearly polarized laser pulse. One can see, that if we leave in the wavefunction only the components with angular momenta $l \geq 10$ the cusp structure disappears and we obtain gaussian transverse distribution. It was suggested in [16], that for the case of the linear polarization, cusp originates from the singularity of the Coulomb continuum wavefunction at zero energy. Absence of the cusp in Figure 6 for $L_{\min} = 10$ suggests, that if we use for the projection operation only the Coulomb continuum wavefunctions with high angular momenta, this singularity somehow disappears, or at least becomes less visible.

A plausible explanation for this fact can be obtained, if we consider in more detail the projection operation we perform to find the ionization probabilities. This projection operation, as we mentioned above, relies on the calculation of the overlap integrals between the TDSE solution and the Coulomb continuum wavefunctions. The Coulomb continuum wavefunction is an object notoriously singular at the point $E = 0$. Overlap integrals naturally inherit this singularity, which, as was suggested in [16], produces cusp in the momentum distribution.

The character of the singularity inherited from the Coulomb continuum wavefunctions may, however, be different for different angular momenta l . One can put forwards arguments showing, that this singularity becomes milder with increasing l . The well-known asymptotic expression for the radial Coulomb continuum wavefunction for $r \rightarrow 0$, $E \rightarrow 0$ is (we use

energy normalization here) [22]:

$$R_{El}(r) \approx \frac{2^{l+1}}{(2l+1)!} r^{l+1} \quad r \rightarrow 0, E \rightarrow 0 \quad (9)$$

This expression, considered as a function of energy, is of course, non-singular. The TDSE solution we obtain, considered as a function of spatial variables, has some finite spatial extension a . It is a known property of the Coulomb wavefunctions [23], that for any a , the small- r asymptotic expression (9) faithfully reproduces $R_{El}(a)$ if angular momentum l is high enough. For such l , substitution of the asymptotic form (9) into the overlap integral is legitimate, and we obtain a result which is non-singular in energy. We can see, therefore, that the overlap integrals between the TDSE solution and the continuum Coulomb wavefunctions become less and less singular with increasing l . This, we believe, is the mechanism, which effectively removes the singularity in the overlap integrals and hence in the momentum distributions, if only high angular momenta are important in the expansion (5) of the wavefunction. This, in particular, is the case of the atomic ionization by a laser pulse with close to circular polarization.

IV. CONCLUSION

We studied evolution of the transverse momentum distribution $W(p_{\perp})$, describing distribution of electron momenta in the direction perpendicular to the polarization plane, with the change of the ellipticity parameter. We saw the gradual change of the character of this distribution from the singular cusp-like distribution for the close to linear polarization, to the smooth gaussian-like structure for the close to circular polarization state.

In the latter case, when the ellipticity parameter $\epsilon \rightarrow 1$ we see, that the tunneling formula (7) becomes quantitatively correct. It does not necessarily mean, that Coulomb effects are completely absent for the circular polarization. It is hardly possible, indeed, that a singular point of a generic function depending on a parameter (ellipticity parameter in the present case) can disappear completely when the parameter gradually changes. We would rather be inclined to believe, that the singularity simply becomes much more difficult to see. Indeed, the Figure 4 shows, that exponent α in Eq. (8) is less than 1 for $\epsilon = 0$. This means, that $W(p_{\perp})$ has infinite first derivative at $p_{\perp} = 0$. At the value of the ellipticity parameter $\epsilon \approx 0.1$, first derivative of $W(p_{\perp})$ ceases to be infinite at $p_{\perp} = 0$. It is the second derivative

of $W(p_{\perp})$ which becomes infinite at this point. The singularity, therefore, becomes milder but does not go away completely. We believe, this is what might happen for $\epsilon = 1$, some higher order derivatives of $W(p_{\perp})$ at the point $p_{\perp} = 0$ are still infinite, which is, of course, very difficult to establish in numerical calculation.

From the practical point of view, the Coulomb effects in the distribution $W(p_{\perp})$ of the electron momenta in the direction perpendicular to the polarization plane become hardly important for the ellipticity parameter as large as 0.8. As we have seen, the tunneling formula (7) works quite reliably for such degree of polarization. The reason for this diminishing of the role of the Coulomb effects can be attributed, we believe, to the mechanism which we described above, and which effectively removes the singularity from the overlaps integrals for the close to circular polarization of the laser pulse.

ACKNOWLEDGMENT

Author acknowledges support of the Australian Research Council in the form of the Discovery grant DP120101805. Author is grateful to Prof. A.S.Kheifets for the stimulating discussions and to a referee for a valuable suggestion. Resources of the National Computational Infrastructure (NCI) Facility were employed.

-
- [1] L. V. Keldysh, *Sov. Phys. -JETP* **20**, 1307 (1965).
- [2] F. H. M. Faisal, *J. Phys. B* **6**, L89 (1973).
- [3] H. R. Reiss, *Phys. Rev. A* **22**, 1786 (1980).
- [4] A. M. Perelomov and V. S. Popov, *Sov. Phys. -JETP* **25**, 482 (1967).
- [5] V. S. Popov, *Physics-Uspekhi* **47**, 855 (2004).
- [6] A. Becker and F. H. M. Faisal, *J. Phys. B* **38**, R1 (2005), URL <http://stacks.iop.org/0953-4075/38/R1>.
- [7] F. H. M. Faisal and G. Schlegel, *J. Mod. Opt.* **53**, 207 (2006).
- [8] D. G. Arbó, J. E. Miraglia, M. S. Gravielle, K. Schiessl, E. Persson, and J. Burgdörfer, *Phys. Rev. A* **77**, 013401 (2008).
- [9] I. Dreissigacker and M. Lein, *Chemical Physics* **414**, 69 (2013).
- [10] N. B. Delone and V. P. Krainov, *J. Opt. Soc. Am. B* **8**, 1207 (1991).
- [11] M. V. Ammosov, N. B. Delone, and V. P. Krainov, *Sov. Phys. -JETP* p. 1191 (1986).
- [12] C. I. Blaga, F. Catoire, P. Colosimo, G. G. Paulus, H. G. Muller, P. Agostini, and L. F. DiMauro, *Nature Physics* **5**, 335 (2008).
- [13] Z. Chen, T. Morishita, A.-T. Le, M. Wickenhauser, X. M. Tong, and C. D. Lin, *Phys. Rev. A* **74**, 053405 (2006).
- [14] T. Brabec, M. Y. Ivanov, and P. B. Corkum, *Phys. Rev. A* **54**, R2551 (1996).
- [15] S. P. Goreslavski, G. G. Paulus, S. V. Popruzhenko, and N. I. Shvetsov-Shilovski, *Phys. Rev. Lett.* **93**, 233002 (2004).
- [16] A. Rudenko, K. Zrost, T. Ergler, A. B. Voitkiv, B. Najjari, V. L. B. de Jesus, B. Feuerstein, C. D. Schröter, R. Moshhammer, and J. Ullrich, *Journal of Physics B: Atomic, Molecular and Optical Physics* **38**, L191 (2005), URL <http://stacks.iop.org/0953-4075/38/i=11/a=L01>.
- [17] A. N. Pfeiffer, C. Cirelli, A. S. Landsman, M. Smolarski, D. Dimitrovski, L. B. Madsen, and U. Keller, *Phys. Rev. Lett.* **109**, 083002 (2012), URL <http://link.aps.org/doi/10.1103/PhysRevLett.109.083002>.
- [18] L. Arissian, C. Smeenk, F. Turner, C. Trallero, A. V. Sokolov, D. M. Villeneuve, A. Staudte, and P. B. Corkum, *Phys. Rev. Lett.* **105**, 133002 (2010).
- [19] I. A. Ivanov, *Phys. Rev. A* **83**, 023421 (2011).

- [20] I. A. Ivanov and A. S. Kheifets, *Phys. Rev. A* **87**, 033407 (2013).
- [21] M. Nurhuda and F. H. M. Faisal, *Phys. Rev. A* **60**, 3125 (1999).
- [22] L. D. Landau and E. M. Lifshitz, *Quantum Mechanics* (Pergamon Press, 1965).
- [23] M. Abramowitz and I. E. Stegun, *Handbook of Mathematical Functions* (National Bureau of Standards, Washington, 1967).

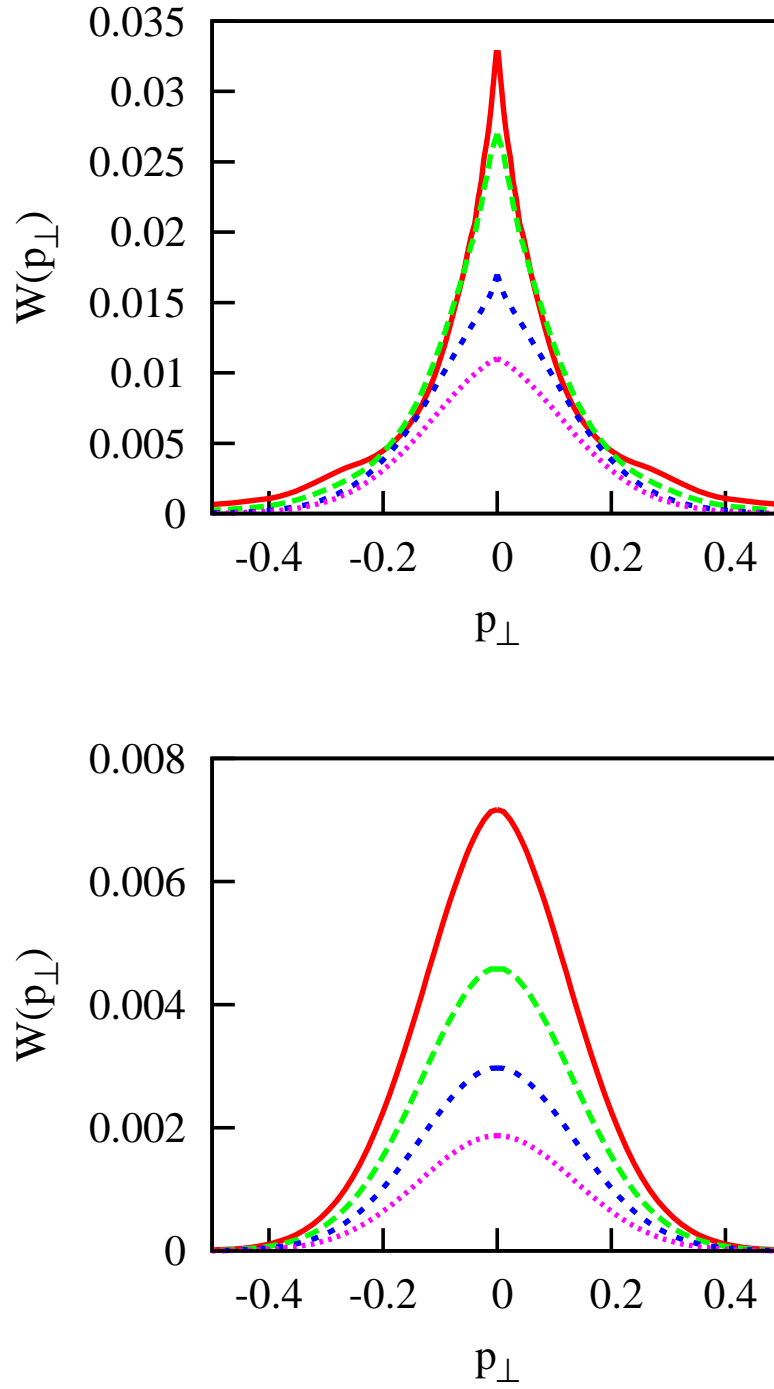


FIG. 1: (Color online) Top panel: distribution $W(p_{\perp})$ for $\epsilon = 0$ (solid (red) line), $\epsilon = 0.2$ (dash (green)), $\epsilon = 0.4$ (short dash (blue)), $\epsilon = 0.5$ (dots (magenta)). Bottom panel: distribution $W(p_{\perp})$ for $\epsilon = 0.6$ (solid (red) line), $\epsilon = 0.7$ (dash (green)), $\epsilon = 0.8$ (short dash (blue)), $\epsilon = 1$ (dots (magenta)). Pulse parameters: $E = 0.0534$ a.u., $\omega = 0.057$ a.u., pulse duration- four optical cycles.

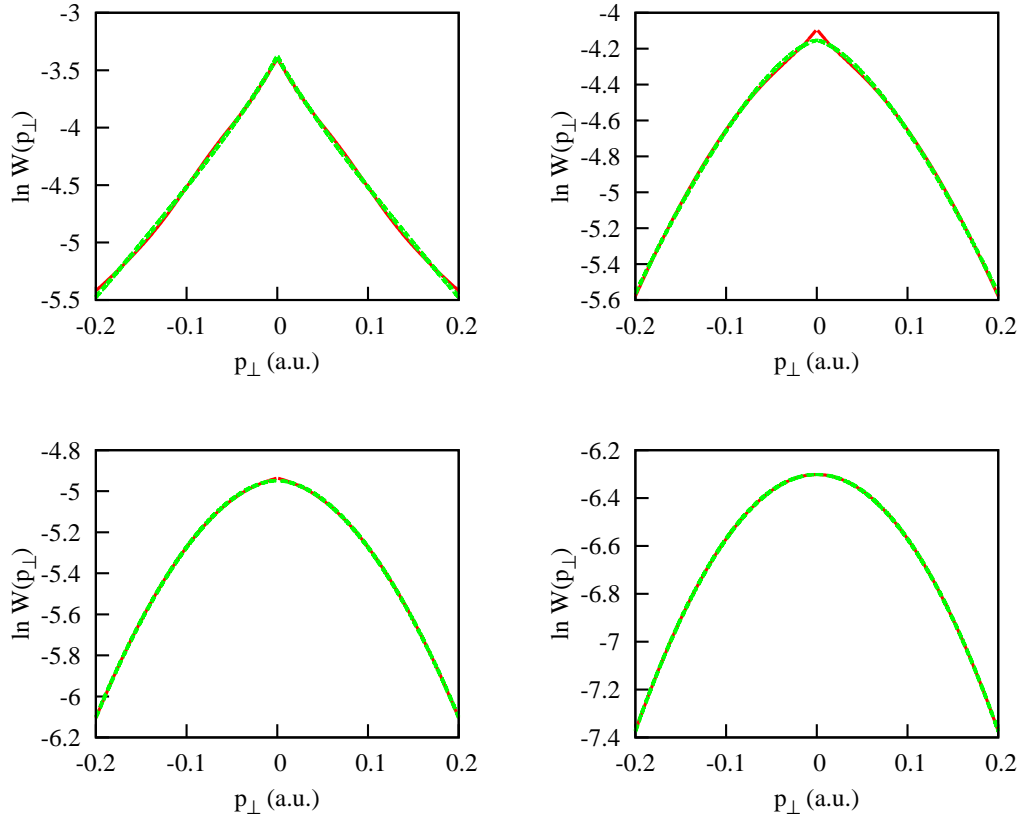


FIG. 2: (Color online) Function $V(p_{\perp}) = \ln W(p_{\perp})$ (red) solid line and results of the fit based on Eq. (8) for $\epsilon = 0, 0.4, 0.6, 1$ (left to right, top to bottom). Pulse parameters: $E = 0.0534$ a.u., $\omega = 0.057$ a.u., pulse duration- four optical cycles.

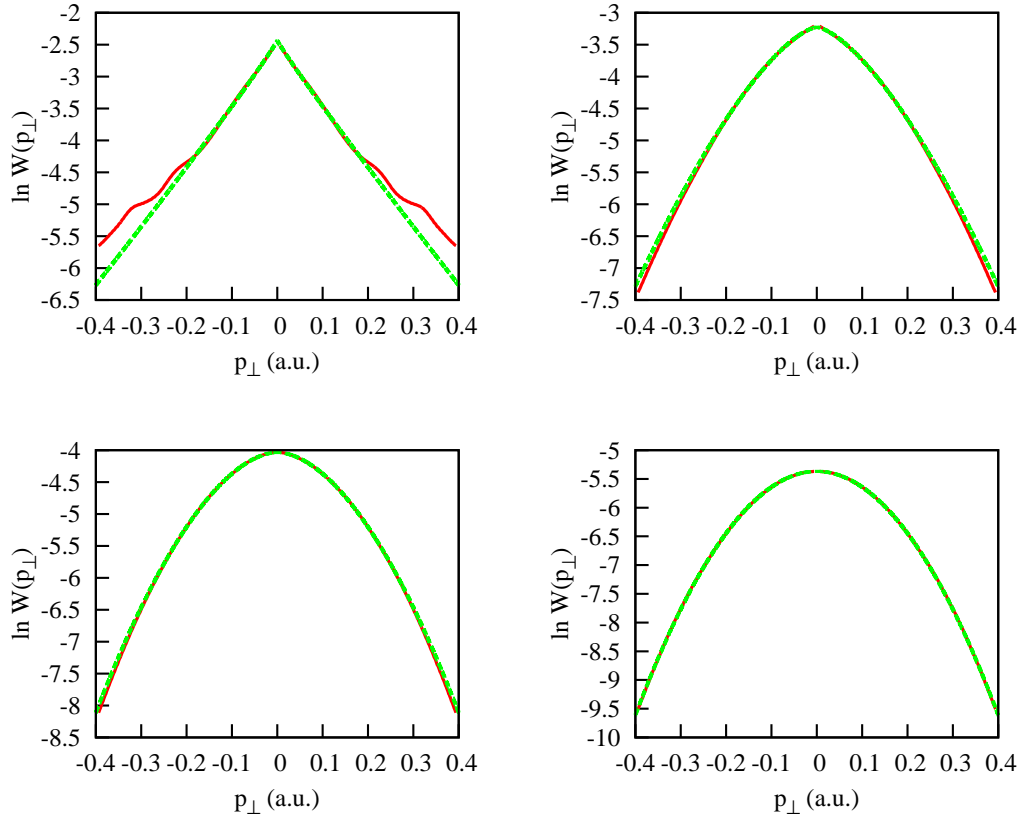


FIG. 3: (Color online) Function $V(p_{\perp}) = \ln W(p_{\perp})$ (red) solid line and results of the fit based on Eq. (8) for $\epsilon = 0, 0.4, 0.6, 1$ (left to right, top to bottom). Pulse parameters: $E = 0.0534$ a.u., $\omega = 0.057$ a.u., pulse duration- ten optical cycles.

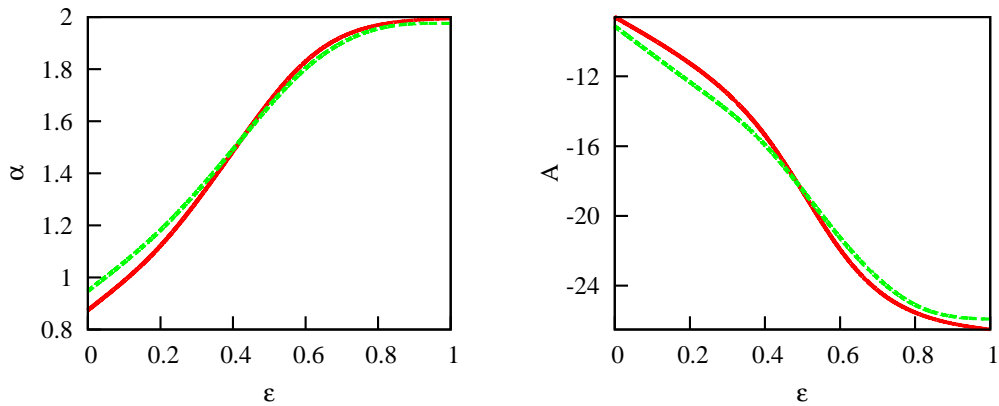


FIG. 4: (Color online) Fitting parameters A and α in Eq. (8) as functions of the ellipticity parameter ϵ . Pulse duration: 4 optical cycles: (red) solid line; 10 optical cycles (green) dash. Other pulse parameters: $E = 0.0534$ a.u., $\omega = 0.057$ a.u.

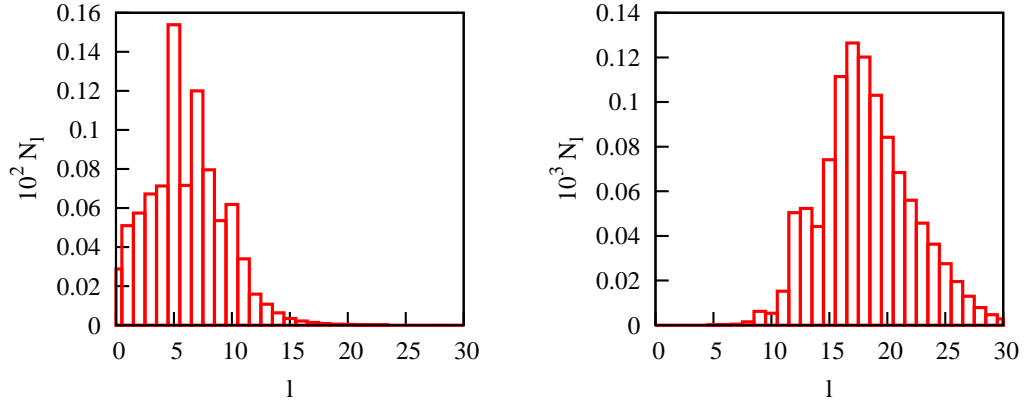


FIG. 5: (Color online) Angular momentum distributions for $\epsilon = 0$ (left panel) and $\epsilon = 0.8$ (right panel). Pulse parameters: $E = 0.0534$ a.u., $\omega = 0.057$ a.u., pulse duration- four optical cycles.

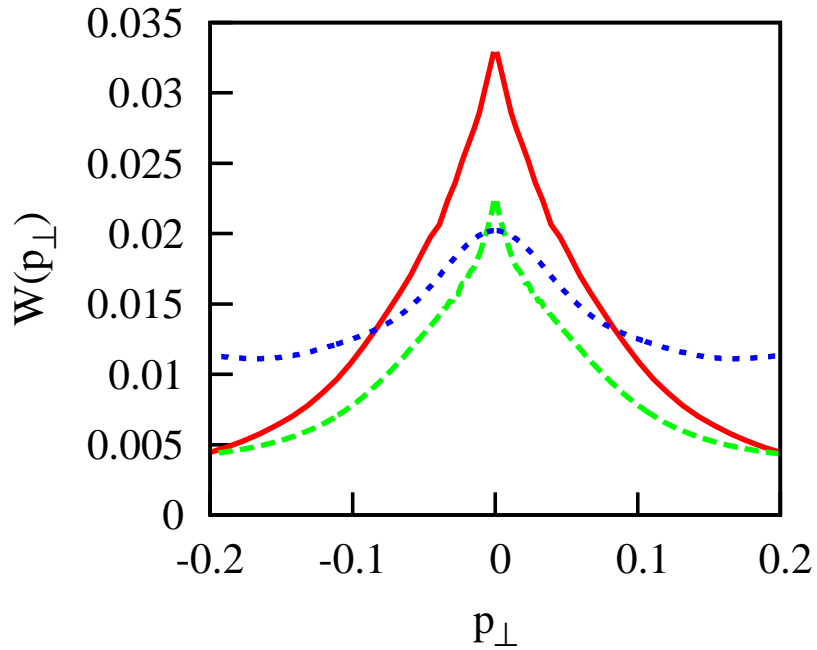


FIG. 6: (Color online) Distribution $W(p_{\perp})$. Projection on the Coulomb scattering states with $L_{\min} = 0$ (solid (red) line), $L_{\min} = 5$ (dash (green)), $L_{\min} = 10$ (short dash (blue)). Distribution for $L_{\min} = 10$ is scaled by a factor of 10 for better visibility. Pulse parameters: $\epsilon = 0$, $E = 0.0534$ a.u., $\omega = 0.057$ a.u., pulse duration- four optical cycles.